SUPPLEMENTAL MATERIAL

***Staphylococcus aureus* CstB is a novel multidomain persulfide dioxygenase-sulfurtransferase involved in hydrogen sulfide detoxification**

Jiangchuan Shen, Mary E. Keithly, Richard N. Armstrong, Khadine A. Higgins, Katherine A. Edmonds and David P. Giedroc

This file contains **Supplementary Methods** and **Supplementary Figures S1-S9**.

Supplementary Methods

NMR spectroscopy. ^{1}H-detected NMR spectra were acquired for the isolated CstB^{Rhod} domain (200 μM) buffer exchanged into 50 mM sodium phosphate, 100 mM NaCl, pH 6.5 at 25 ºC on a 600 MHz Agilent DDR spectrometer equipped with cryogenic probe system in the METACyt Biomolecular NMR Laboratory. For the ^{1}H-^{1}H NOESY, a mixing time (t_m) of 150 ms was used, with 32 scans per t_2 increment.

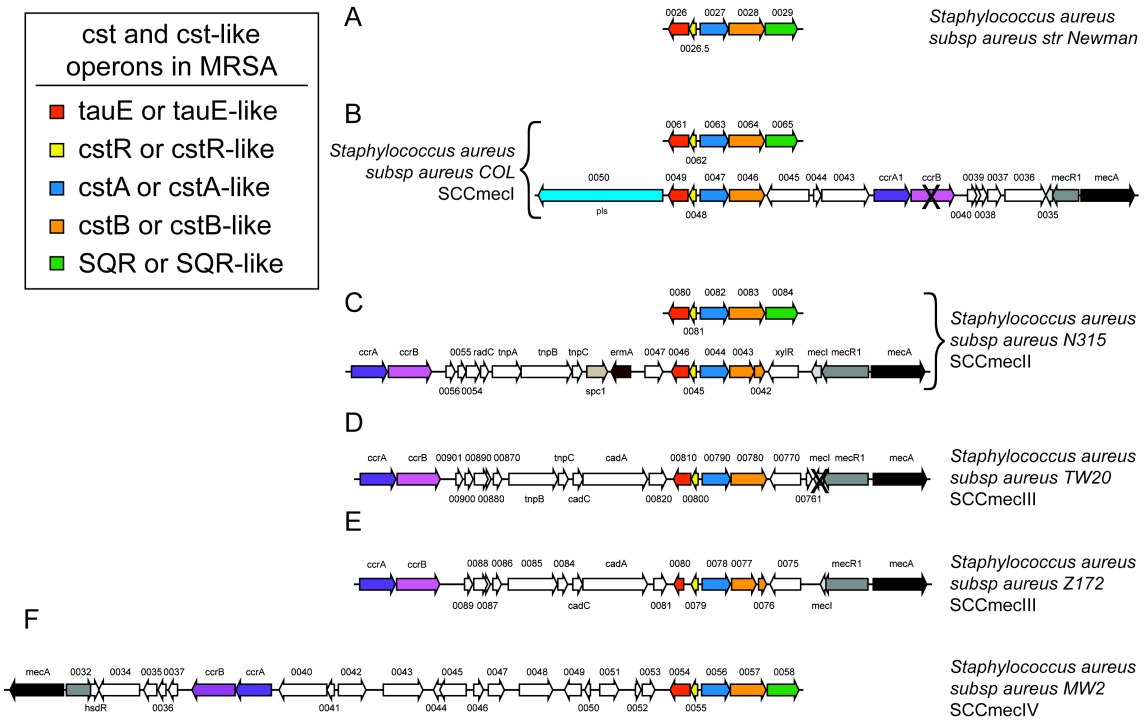

Supplementary Figure S1. Chromosomal gene arrangement of *cst* and *cst*-like operons in various strains of *Staphylococcus aureus* reveals that *cst*-like operons are frequently associated with methicillin resistance genes. *Cst* operon encoded genes are shaded as shown in the *inset*. Staphylococcal cassette chromosome *mec* elements (SCCmec) encode the methicillin resistance gene *mecA* (*black*), usually along with a full or truncated version of the signal transducer protein *mecR1* (*gray*), and the repressor *mecI* (*light gray*). SCCmecs also contain cassette chromosome recombinases, *e.g., ccrA* and *ccrB* (shaded in *dark* and *light purple*, respectively). Additionally, SCCmecs contain variable, joining regions that typically include a variety of other resistance determinants; examples include the erythromycin resistance gene *ermA* (*brown*), *spc1* (*tan*) that mediates resistance to spectomycin and streptomycin, and the methicillin-resistant surface protein *pls* (*cyan*). (A) The organization of the *cst* operon in the methicillin-sensitive (MSSA) Newman strain from which CstB studied in this work is derived. No other *cst*-like operon is found in this and many other MSSA strains. (B) The *cst* operon in the methicillin-resistant (MRSA) COL strain (*top*) along with a similar operon containing homologs of *tauE*, *cstR*, *cstA*, and *cstB* within a typeI CCmec (*bottom*). (C) The organization of the *cst* operon and a *cst*-like operon within a typeII SCCmec in the MRSA N315 strain. In this *cst*-like operon, the *cstB*–like genes appear to encode a rhodanese homology domain (0042) that is separate from the PDO-Rhod fusion (0043). (D) The organization of a *cst*-like operon with an intact *cstB*-like gene within a typeIII SCCmec in the MRSA TW20 strain*. (E) The organization of a *cst*-like operon with a split *cstB*-like gene within a typeIII SCCmec in the Z172 strain*. (F) The organization of a *cst* operon near the type IV SCCmec in the MRSA MW2 strain. *No other bona-fide *cst* operon is found in the TW20 and Z172 strains. This figure was produced using SyntTax.[1]

We observe here that type I, type II, and typeIII SCCmec elements frequently contain a *cst*-like operon containing a one- or two-part *cstB*-like gene. We also observe that the strain MW2, which

has a type IV SCCmec, has a complete *cst* operon very near the *ccrAB* and *mec* complexes. In some cases, as in the COL strain (type I) (panel B) or the N315 strain (type II) (panel C), the *cst*-like operon is present in addition to the complete *cst* operon originally described in S. aureus strain Newman (panel A),[2] while in other strains the operon in or near the SCCmec appears to be the only *cst*-like operon in the genome (panels D and E). We speculate that the presence of a *cst*-like operon alongside so many variations of the methicillin resistance genes indicates that the proteins encoded by these genes may enhance or contribute in some way to antibiotic resistance or virulence.

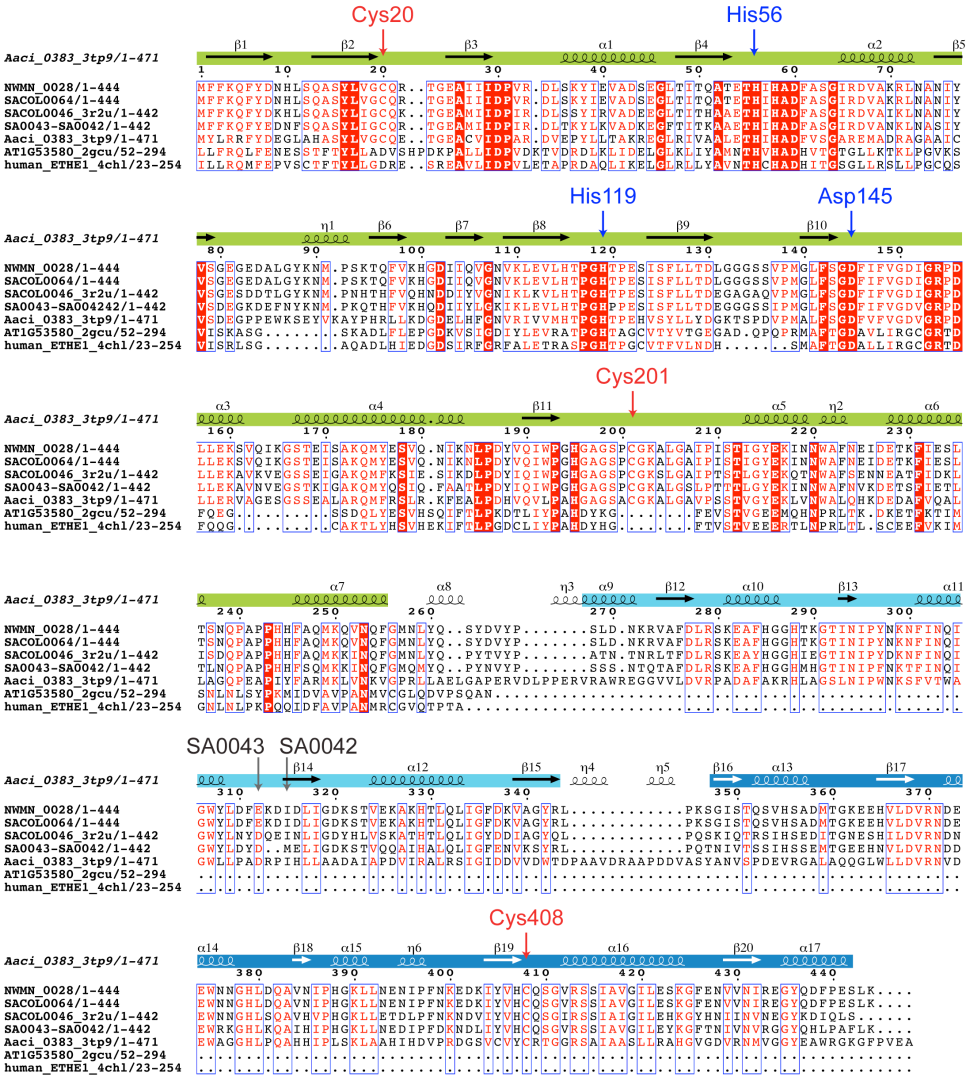

Supplemental Figure S2. Structure-based sequence alignment of CstB with other persulfide dioxygenases. Amino acid sequence alignment of CstB and homologs, including CstBs from the *S. aureus* strain Newman (NWMN_0028) studied in this work, and COL (SACOL0064), as well as a CstB from the duplicated core *cst* operon (SACOL0046), and a split CstB from the duplicated core cst operon from the *S. aureus* strain N315 (SA0043-SA0042) (see Fig. S1B &

S1C). Additional homologs with known crystal structures are also included, from *A. acidocaldarius* (Aaci_0383; PDB 3TP9), the ETHE1-like protein from *Arabidopsis thaliana* (AT1G53580; pdb 2GCU)[3] and human ETHE1 (PDB 4CLH).[4] Secondary structural elements from the *A. acidocaldarius* crystal structure (PDB 3TP9) are shown above the sequence with these elements derived from the core ETHE1-like PDO, middle RHD and C-terminal Rhod domains shaded *green*, *cyan* and *blue*, respectively. *Red* arrows mark the crucial cysteine residues C20, C201, and C408 investigated in this work. *Blue* arrows indicate the H56, H119, and D145 residues responsible for coordinating Fe(II) (see Fig. 2B, main text). Gray arrows mark the C-terminus of SA0043 and the N-terminus of SA0042. The structure-based alignment was generated using PROMALS3D[5] and rendered using ESPript 3.[6]

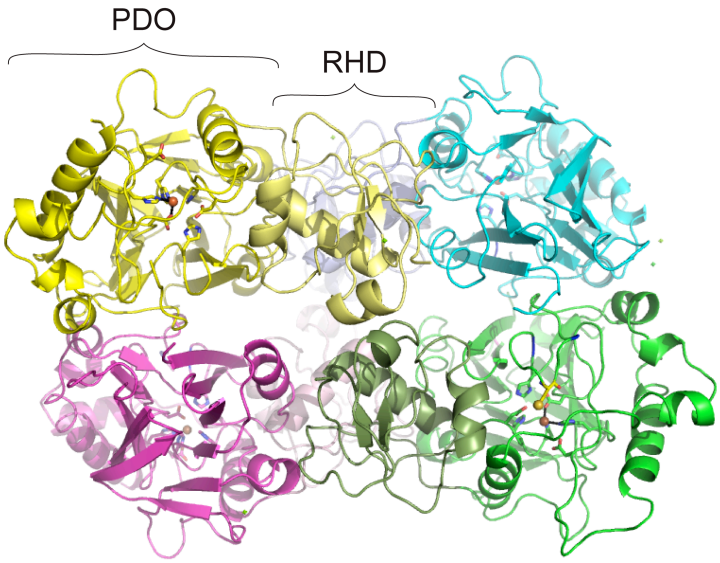

Supplementary Figure S3. CstB2 crystal structure asymmetric unit suggests likely tetramer interfaces. Ribbon representation of the D_2-symmetric CstB2 tetramer with each subunit shaded differently. The N-terminal PDO domain (residues 1-256) is shaded darker than the corresponding rhodanese homology domain (RHD; residues 257-246), which mediates most of the intersubunit contacts in the crystal structure.

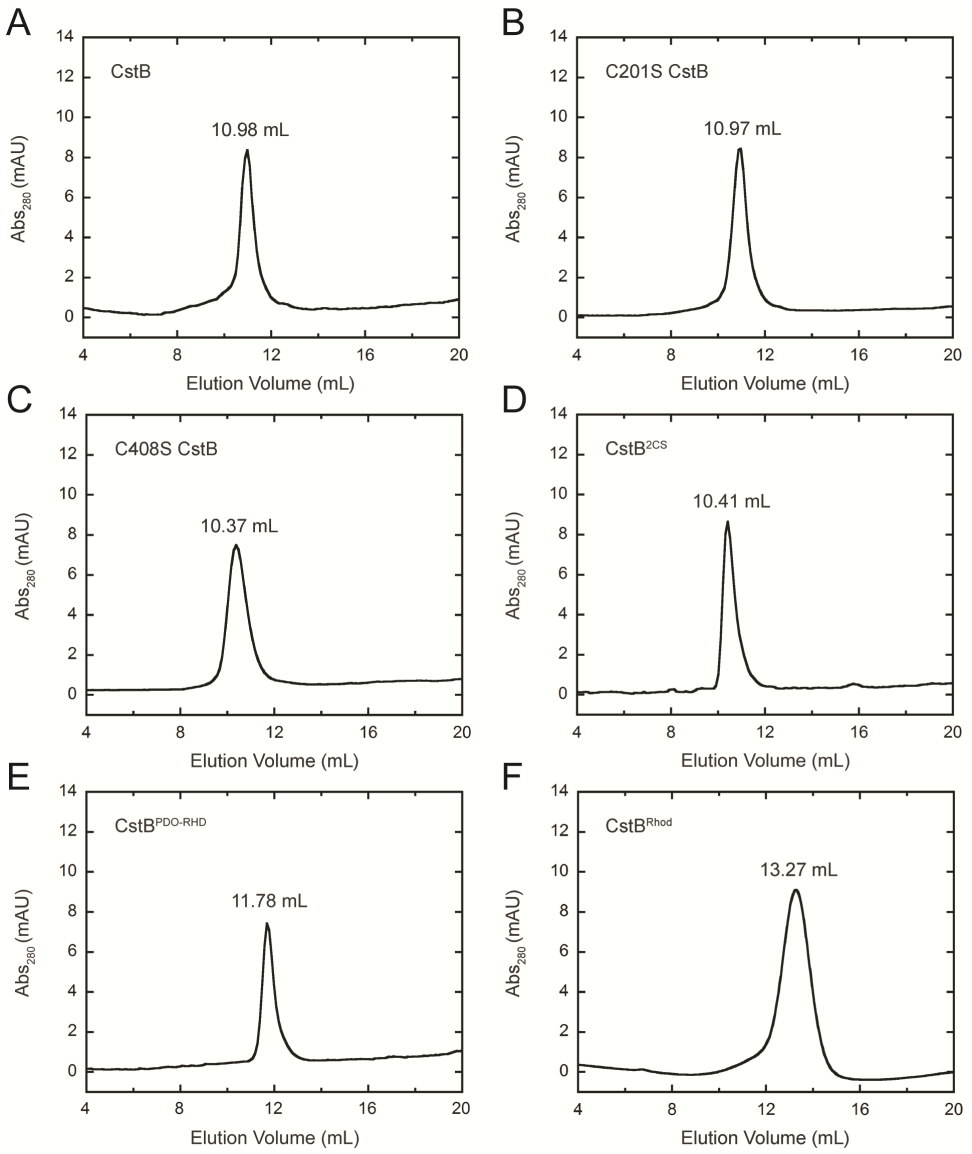

Supplementary Figure S4. Gel filtration profiles for wild-type CstB, missense mutant CstBs and domain fragments of CstB. Gel filtration profiles of (A) wild-type CstB, V_e= 10.98 mL; (B) C201S CstB, V_e= 10.97 mL; (C) C408S CstB, V_e= 10.37 mL; (D) C2S CstB, V_e= 10.41 mL and (E) $CstB^{PDO\text{-}RHD}$, V_e= 11.78 mL were obtained from a Superdex-200 Increase gel filtration column and (F) $CstB^{Rhod}$, V_e= 13.27 mL from a Superdex-75 gel filtration column. The standards used for Superdex-200 Increase gel filtration column were ovalbumin (44 kDa), conalbumin (75 kDa), aldolase (158 kDa), ferritin (440 kDa) and thyroglobulin (669 kDa). The standards used for the Superdex-75 gel filtration column were aprotinin (6.5 kDa), ribonuclease A (13.7 kDa), chymotrypsinogen (25 kDa), ovalbumin (44 kDa) and conalbumin (75 kDa). Buffer conditions: 25 mM Tris, 100 mM NaBr, 5 mM DTT, pH 8.0. See Table 1, main text for apparent molecular weights.

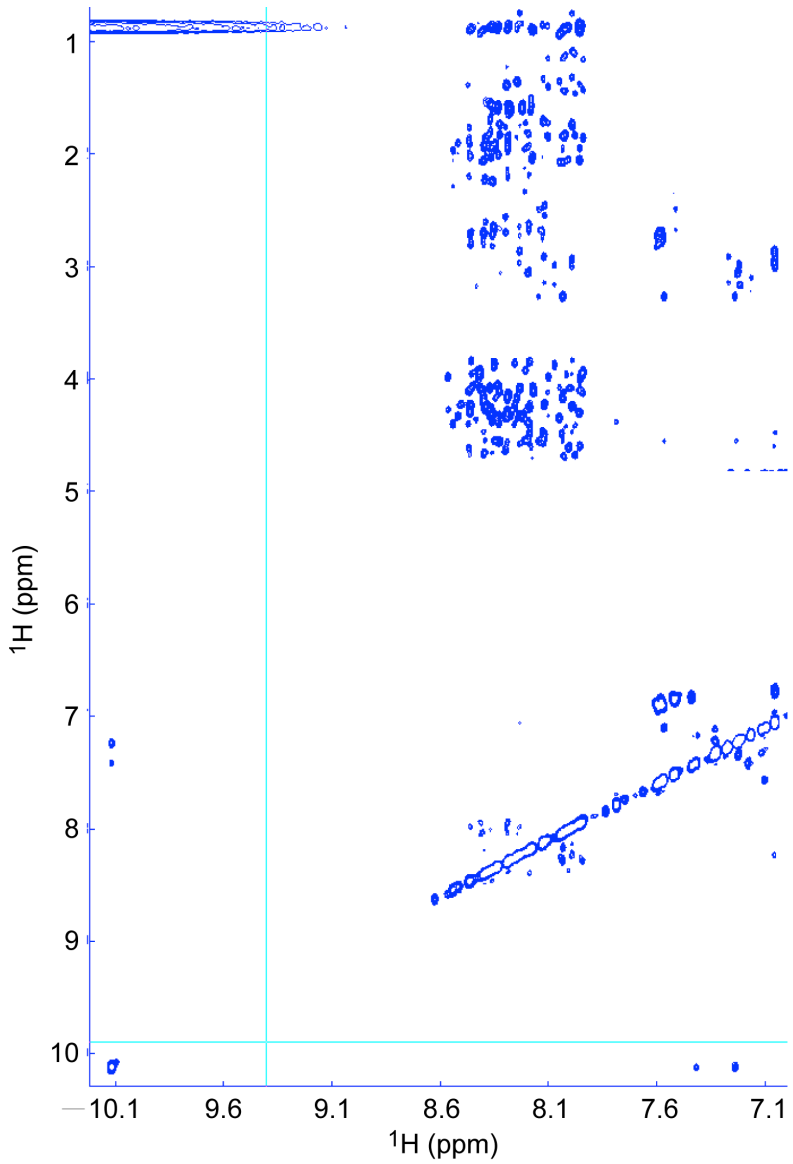

Supplementary Figure S5. Sub-region of the ^{1}H-^{1}H NOESY spectrum of CstB^{Rhod} highlighting amide-aliphatic NOEs. Most observable crosspeaks are found in the "random-coil" region of the spectrum, δ=7.6-8.5 ppm. No amide crosspeaks from stable α- or β- structure appear in this spectrum and there is essentially no dispersion in the methyl ^{1}H region (*top*), all findings incompatible with a well-folded and monomeric ≈11 kDa protein. Conditions: 25 ºC, pH 6.5, t_m=150 ms, 600 MHz spectrometer.

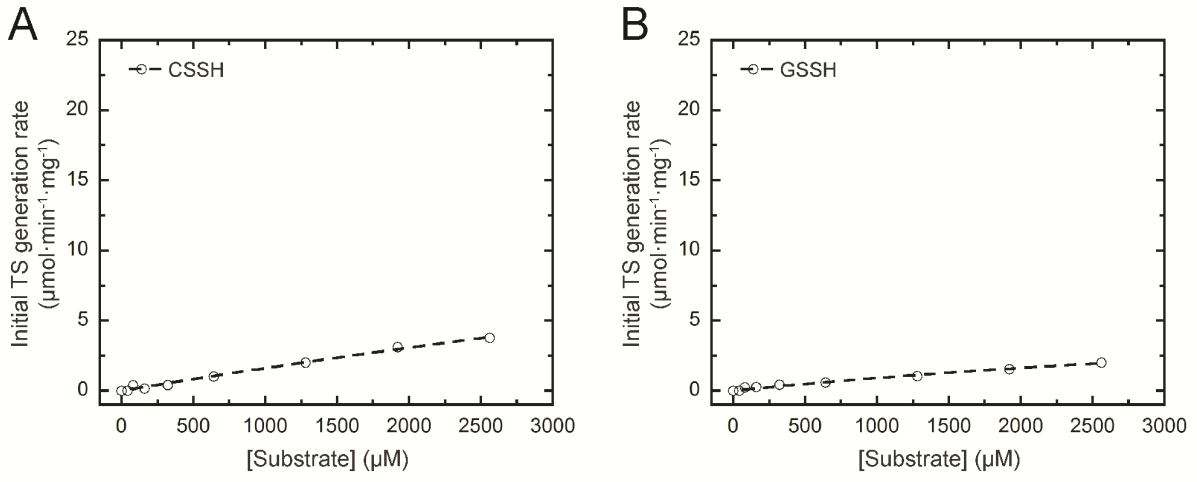

Supplementary Figure S6. Coupled persulfide dioxygenase-persulfide transferase (cPDO-PT) activity of CstB with alternative persulfide substrates. (A) Initial TS generation rates as a function of the concentration of CSSH (*open circles*) and the *dashed*, continuous line through the open circles is a fit to the Michaelis-Menten equation, with parameters summarized in Table 2, main text. (B) Initial TS generation rates as a function of the concentration of GSSH (*open circles*) and the *dashed*, continuous line through the open circles is a fit to the Michaelis-Menten equation, with parameters summarized in Table 2, main text.

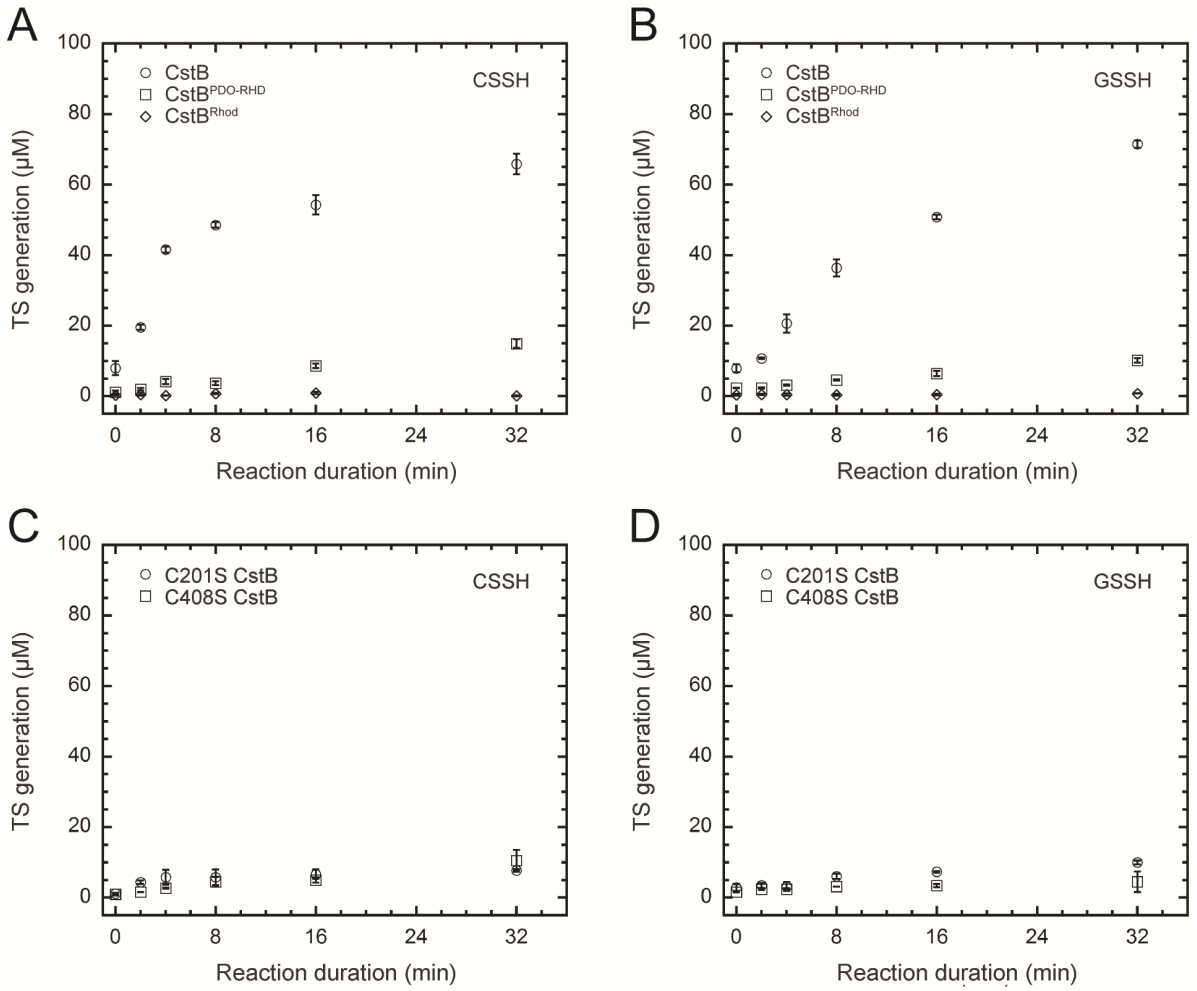

Supplementary Figure S7. **Coupled persulfide dioxygenase-persulfide transferase (cPDO-PT) activities for wild-type CstB, domain fragments of CstB and missense mutant CstBs with alternative persulfide substrates.** (A) TS generation from 200 μM CSSH substrate as a function of reaction duration in the presence of 10 μM wild-type CstB (*open circles*), $CstB^{PDO-RHD}$ (*open squares*) and $CstB^{Rhod}$ (*open diamonds*). (B) TS generation from 200 μM GSSH as a function of reaction duration in the presence of 10 μM wild-type CstB (*open circles*), $CstB^{PDO-RHD}$ (*open squares*) and $CstB^{Rhod}$ (*open diamonds*). (C) TS generation from 200 μM CSSH as a function of reaction duration in the presence of 10 μM C201S CstB (*open circles*), and C408S CstB (*open squares*). (D) TS generation from 200 μM GSSH as a function of reaction duration in the presence of 10μM C201S CstB (*open circles*) and C408S CstB (*open squares*).

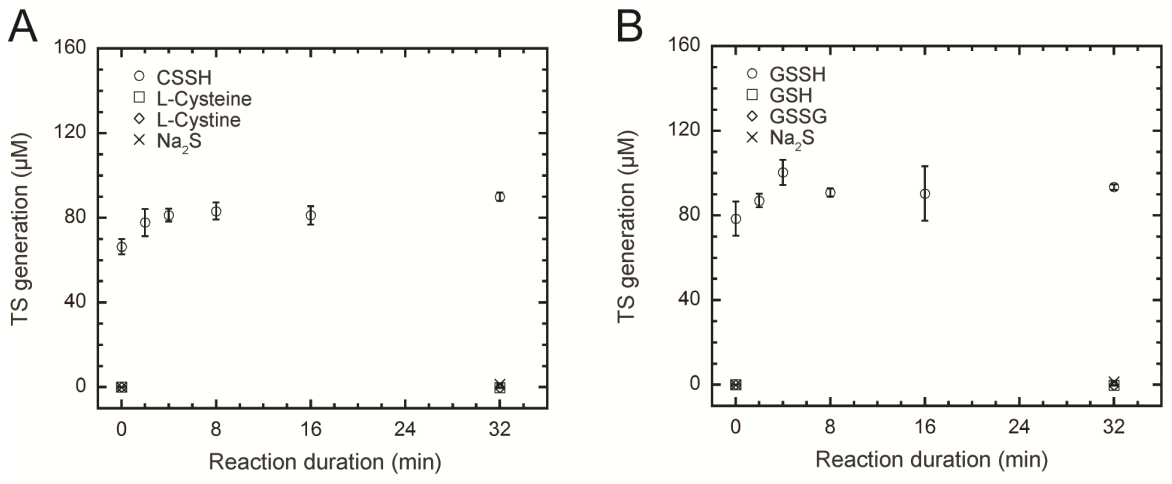

Supplementary Figure S8. Representative time-course kinetics indicating LMW persulfide substrates react with sulfite to generate TS non-catalytically. (A) Kinetics of non-catalyzed TS generation resulting from mixing 200 μM sulfite with 200 μM CSSH (*open circles*) vs. *L*-cysteine (*open squares*), *L*-cystine (*open diamonds*) and Na_2S (*crosses*). (B) Kinetics of non-catalyzed TS generation resulting from mixing 200 μM sulfite and 200 μM GSSH (*open circles*) vs. GSH (*open squares*), GSSG (*open diamonds*) and Na_2S (*crosses*).

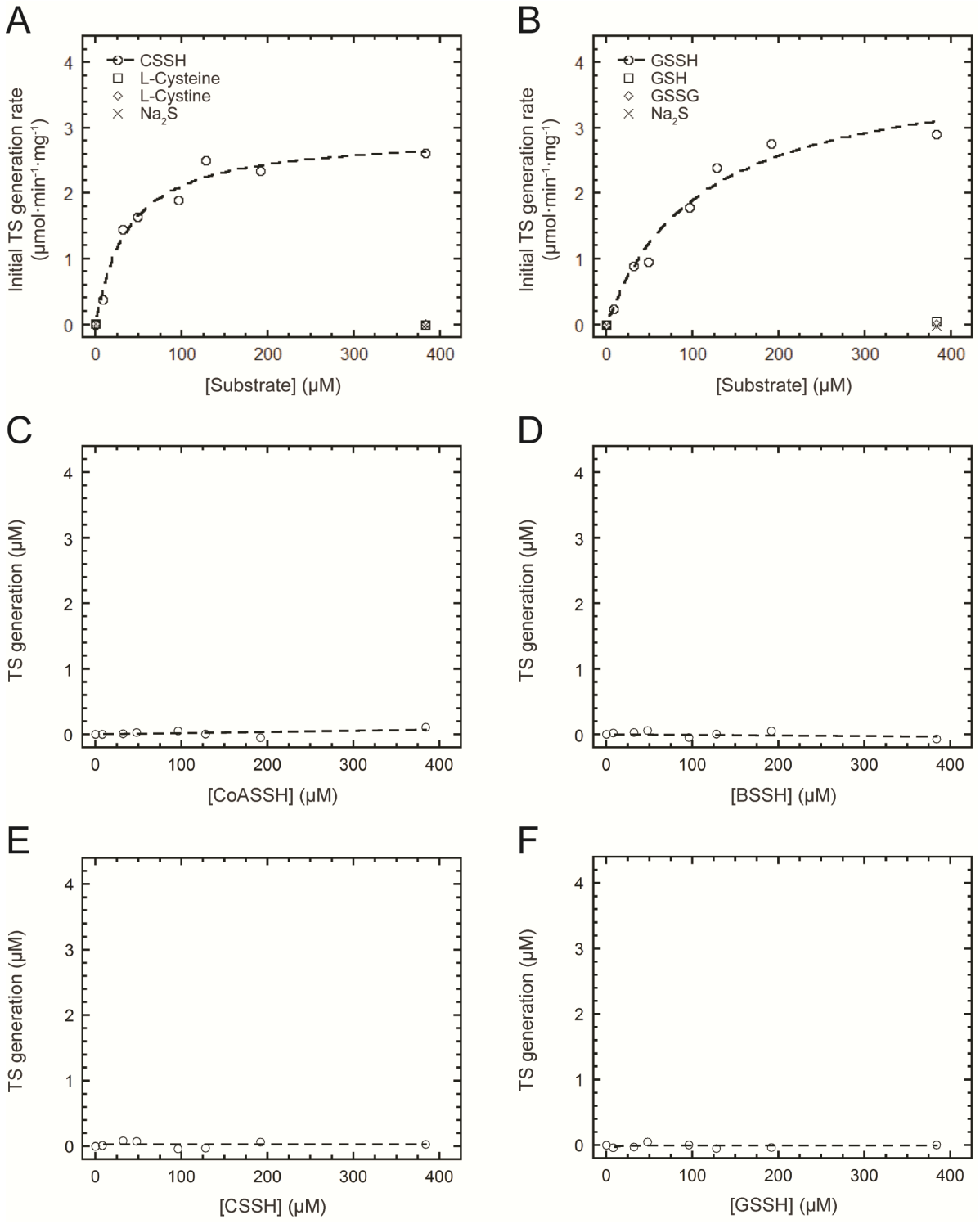

Supplementary Figure S9. C201S CstB displays persulfide transferase (PT) activity with other LMW persulfide substrates (A-B) and CstB^{2CS} (C-F) displays no significant activity with any LMW persulfide substrate tested. (A) Initial TS generation rates as a function of the

concentrations of CSSH (*open circles*) vs. *L*-cysteine (*open squares*), *L*-cystine (*open diamonds*) and Na_2S (*crosses*) for C201S CstB. The *dashed*, continuous line through the open circles is a fit to the Michaelis-Menten equation, with parameters summarized in Table 3, main text. (B) Initial TS generation rates as a function of the concentrations of GSSH (*open circles*) vs. GSH (*open squares*), GSSG (*open diamonds*) and Na_2S (*crosses*) for C201S CstB. The *dashed*, continuous line through the open circles is a fit to the Michaelis-Menten equation, with parameters summarized in Table 3, main text. (C) Initial TS generation rates for $CstB^{2CS}$ as a function of the concentration of CoASSH (*open circles*) with the *dashed*, continuous line through the open circles is a fit to the Michaelis-Menten equation. (D) Initial TS generation rates for $CstB^{2CS}$ as a function of the concentration of BSSH (*open circles*) and the *dashed*, continuous line through the open circles is a fit to the Michaelis-Menten equation. (E) Initial TS generation rates for $CstB^{2CS}$ as a function of the concentration of CSSH (*open circles*) and the *dashed*, continuous line through the open circles is a fit to the Michaelis-Menten equation. (F) Initial TS generation rates for $CstB^{2CS}$ as a function of the concentration of GSSH (*open circles*) and the *dashed*, continuous line through the open circles is a fit to the Michaelis-Menten equation.

REFERENCES

(1) Oberto, J. (2013) SyntTax: a web server linking synteny to prokaryotic taxonomy. *BMC Bioinformatics 14*, 4.

(2) Grossoehme, N., Kehl-Fie, T. E., Ma, Z., Adams, K. W., Cowart, D. M., Scott, R. A., Skaar, E. P., Giedroc, D. P. (2011) Control of copper resistance and inorganic sulfur metabolism by paralogous regulators in Staphylococcus aureus. *J Biol Chem 286*, 13522-13531.

(3) McCoy, J. G., Bingman, C. A., Bitto, E., Holdorf, M. M., Makaroff, C. A., Phillips, G. N., Jr. (2006) Structure of an ETHE1-like protein from Arabidopsis thaliana. *Acta Crystallogr D Biol Crystallogr 62*, 964-970.

(4) Pettinati, I., Brem, J., McDonough, M. A., Schofield, C. J. (2015) Crystal structure of human persulfide dioxygenase: structural basis of ethylmalonic encephalopathy. *Hum Mol Gen, 24,* 2458-2469.

(5) Pei, J., Kim, B. H., Grishin, N. V. (2008) PROMALS3D: a tool for multiple protein sequence and structure alignments. *Nucleic Acids Res 36*, 2295-2300.

(6) Robert, X., Gouet, P. (2014) Deciphering key features in protein structures with the new ENDscript server. *Nucleic Acids Res 42*, W320-324.